9 Simulation of Pull Tests for Grouted Cable Anchors

9.1 Problem Statement

The most common method for determination of cable bolt properties is to perform pull-out tests on small segments of grouted cables in the field. Typically, segments from 10 to 50 cm in length are grouted into boreholes. The ends of these segments are pulled with a jack mounted to the surface of the tunnel and connected to cable via a barrel-and-wedge type anchor. The force applied to the cable, and the deformation of the cable, are plotted to produce an axial force-deflection curve. From this curve, the peak shear strength of the grout bond is determined and converted to a strength in tons/m cable length.

The results for pull tests on one-half meter segments of several types of cables are illustrated in Figure 9.1. These plots are expressed in terms of tons/m versus deformation in mm. For all cables, a water/cement ratio of one-third was used.

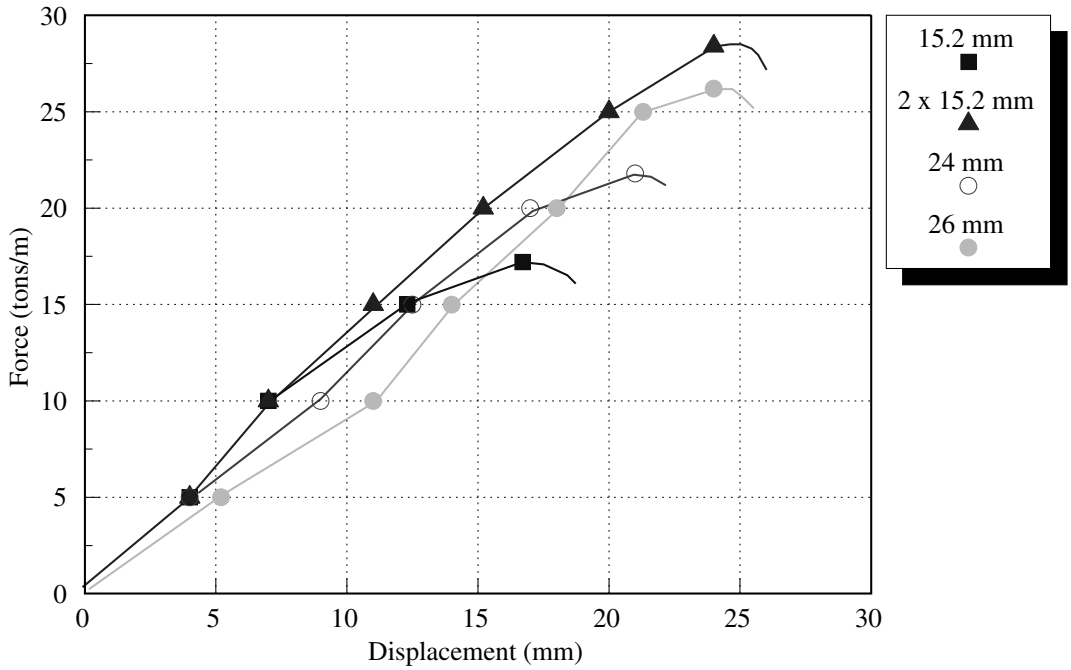

Figure 9.1 Field results for pull tests on various types of cables for a bond length of 0.5 m and a water/cement ratio of 1/3

The properties of typical concrete-reinforcing tendons are given in Table 9.1:

Table 9.1 Typical stranded cable properties

Nominal diameter (mm)	Nominal mass (kg/m)	Nominal area (mm^2)	Grade	Force (kN) at the following % of ultimate tensile strength 55%	65%	75%	100%
15	1.54	177	Super	105	125	145	190
19	2.42	283	Super	170	200	230	305
23	3.49	415	Reg	235	280	325	430
			Super	250	295	340	450
26	4.43	530	Reg	300	355	410	545
			Super	315	370	430	570
29	5.48	660	Reg	375	440	510	680
			Super	390	460	535	710
32	6.64	804	Reg	455	540	625	830
			Super	480	565	655	870
35	7.91	962	Reg	545	645	745	990
			Super	570	675	780	1040
38	9.29	1140	Reg	645	765	880	1175
			Super	675	800	925	1230

In this example problem, *FLAC* is used to model the previous tests and reproduce the field data. It is noted that the current cable bolt model in *FLAC* describes the response of the cable-rock interaction as cohesive and frictional in nature. The model assumes the grout behaves as an elastic, perfectly plastic material with confining stress dependence, but no loss of strength after failure. Recent field and laboratory work (e.g., Kaiser et al. 1992) has shown that dilation introduced by the spiral cable strands can be an important factor in cable response. This behavior is not addressed here, but could be accounted for through the use of a *FISH* routine. More complex behavior can also be simulated using the rockbolt model in *FLAC*. See Section 1.6.4.1 in **Structural Elements** for example pullout tests using rockbolt elements.

9.2 Modeling Procedure

First, we consider the case where the confining stress dependence on the cable shear-bond strength may be neglected. The cable properties required by *FLAC*'s cable-bolt model must be extracted from the field pull-test curve. This is easily done when the field test data are presented in terms of force/unit length versus deformation, as shown in Figure 9.1. Assuming no yielding in the cable, the value of the grout shear stiffness, **kbond**, is simply the slope of the curve, with the ultimate bond strength, **sbond**, being the peak-pull strength value per unit length.

For example, all of the pull-test results shown here have roughly the same loading slope; so, an average value of **kbond** is chosen for all:

$$\textbf{kbond} \approx \frac{28 \text{ tons/meter}}{25 \times 10^{-3}\text{meter}} = 1.12 \times 10^{7} \text{ N/m/m}$$

This value of **kbond** is very low, indicating a rather poor grouting job for the cable. Typical **kbond** values would be approximately one order of magnitude or more higher than this.

The value of **sbond** for the single 15.2 mm wire is simply the peak shear resistance in tons/m. In this case, **sbond** $\approx$ 17.5 tons/m, or 17.5×10^4 N/m. To check this value of **sbond** for reasonableness, it can be converted to grout shear strength by dividing by the approximate surface area of the wire (assuming the bond fails at the grout/cable interface). We find that the peak shear strength is 3.66 MPa. This value should equal roughly half the uniaxial compressive strength of the grout, indicating either a very poor grout or that the cable was allowed to rotate during the pull test, yielding artificially low grout shear-strength values.*

The cable end-node ispulled at a small, constant y-oriented velocity (Figure 9.2). A *FISH* function, **`ff`**, is used to sum the reaction forces and monitor nodal displacement generated by the pull tests for comparison to field test results. See "pull.prj" for a description of the pull test simulation.

---

* This effect is explored in some detail in Hyett et al. 1992.

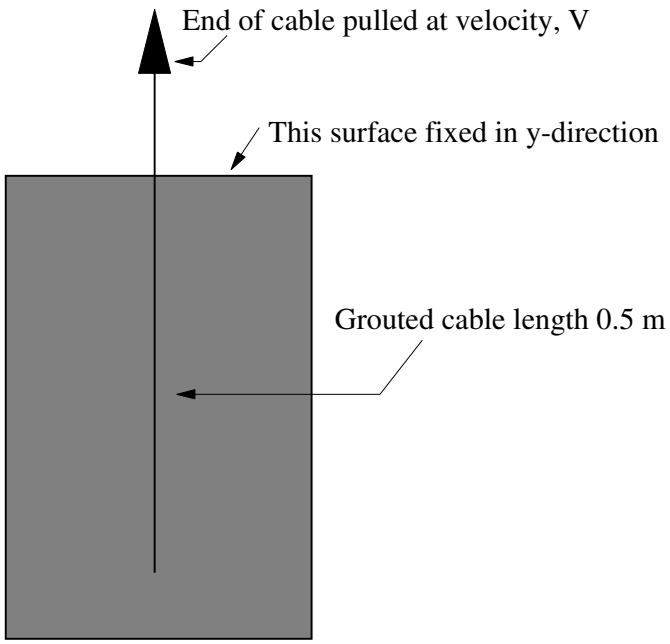

Figure 9.2 Schematic of geometry of FLAC model for a pull test

A plot of history 1 versus history 2 (pull force versus cable displacement) for the case of a single 15.2 mm cable is shown in Figure 9.3. This figure illustrates the general force-displacement behavior given in Figure 9.1. The peak force is reached at a displacement of approximately 17 mm. After this point, the cable is simply pulled out of the borehole in much the same fashion as a block sliding on a plane. Figures 9.4(a-c) show the axial force distribution on the cable for displacements of 10 mm, 17 mm and 17.5 mm, respectively. Superimposed on the axial forces are locations at which the grout bond is yielding. At 10 mm [Figure 9.4(a)], the grout bond has not failed. At 17 mm [Figure 9.4(b)], bond failure is initiated and rapidly propagates [Figure 9.4(c)] down the entire cable length. At that stage, the force on the cable end is simply the sum of **sbond** $\times l_i$ (where l_i is the length of cable segments) for all n-slipping segments. If the embedded length were long enough, the cable axial force would eventually reach the yield force limit of the cable itself. The cable should then break when the extension strain equals the ultimate breaking strain of the cable (generally, around 3%). The cable model does not have an extension strain limit; the rockbolt model (see Section 1.6 in **Structural Elements**) should be used to simulate this condition.

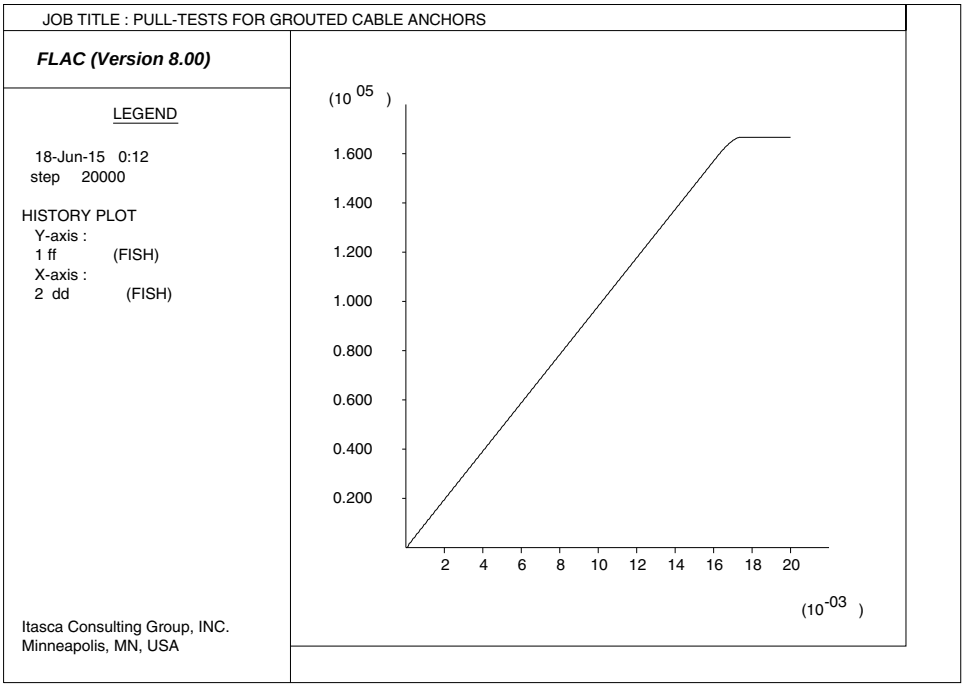

Figure 9.3 Cable pull force in N/m versus cable displacement in meters for the case of a single 15.2 mm grouted cable

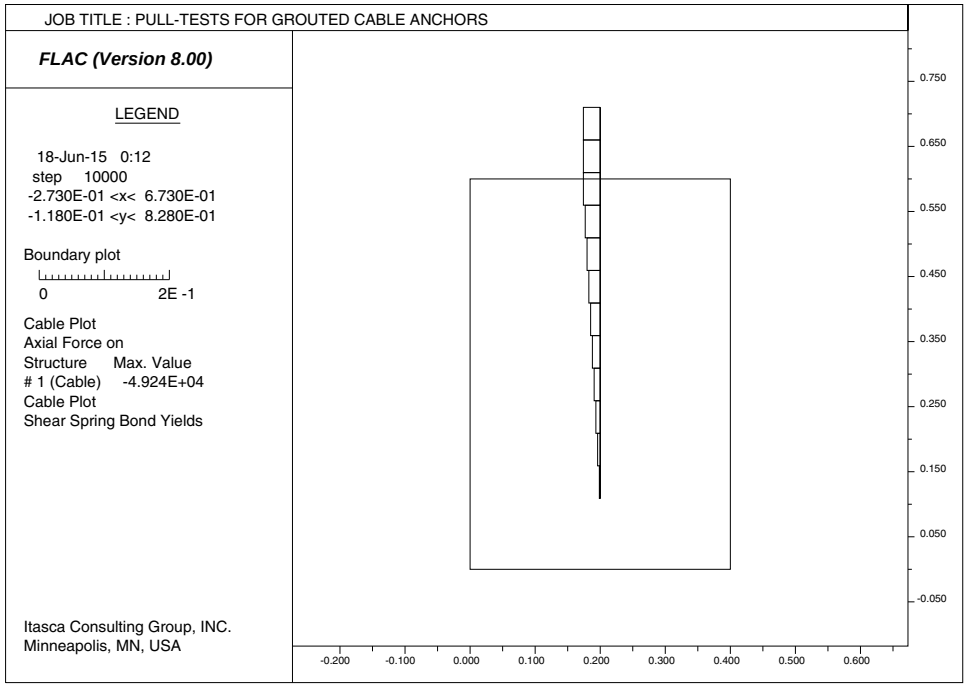

(a) at 10 mm deformation

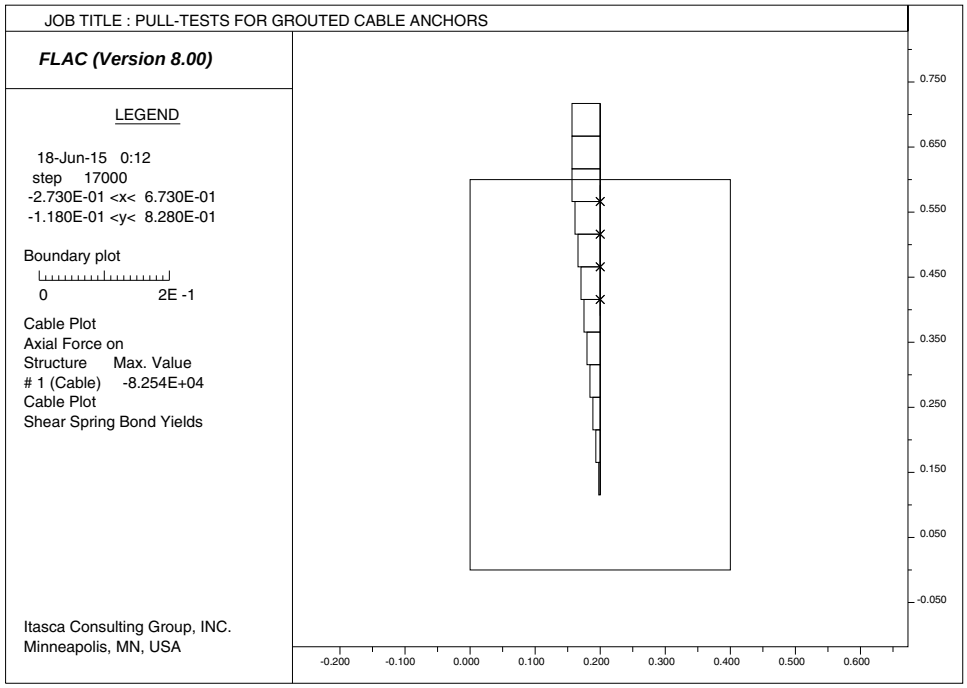

(b) at 17 mm deformation

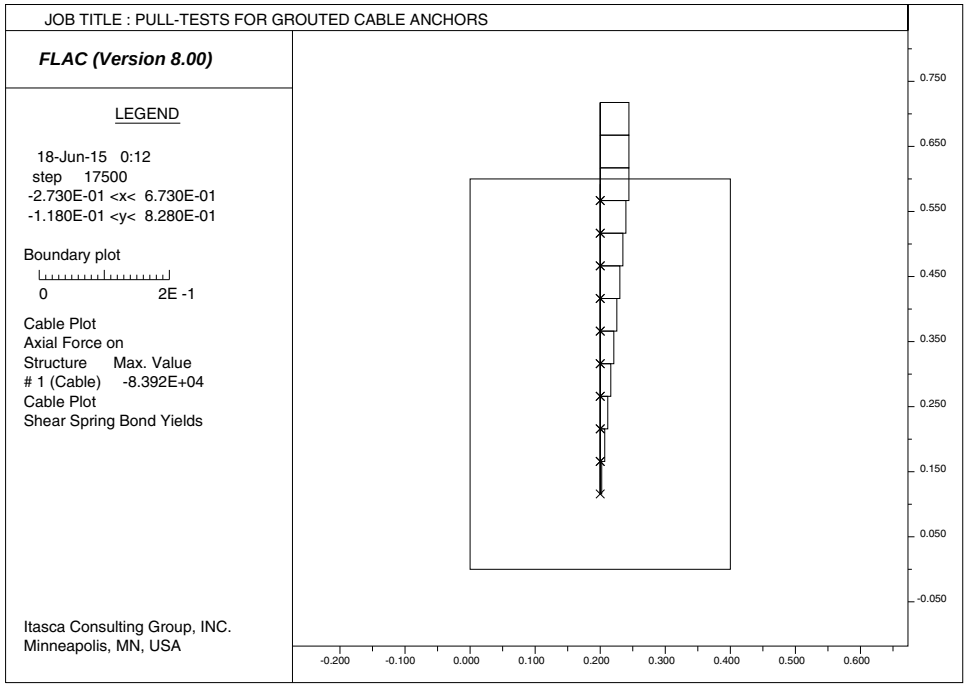

(c) at 17.5 mm deformation

Figure 9.4 ***Plot of axial force and cable bond yield points for pull-test simulation on a 15.2 mm cable bolt. (Note that cable-bond-slip progresses rapidly after peak strength is reached at the first cable element.)***

The evolution of the force profile along the cable is illustrated for the case of the 26 mm cables (Figure 9.5). Here, the force-displacement profiles for various "snapshots" in displacement are compared. Table 10 is labeled 5 mm displacement, and the remaining tables are labeled at 5 mm increments up to 30 mm. (Note that the last three values in each table are for structural nodes outside the grid, and should be neglected.) Up to the point of approximately 20 mm, bond slippage does not occur, and the increase in axial load is essentially elastic. However, bond slippage occurs rapidly between 20 and 25 mm (Tables 40 and 50), with a constant force distribution thereafter. The slope of the final curve is approximately **sbond**/L, where L is the initial grouted length of the cable.

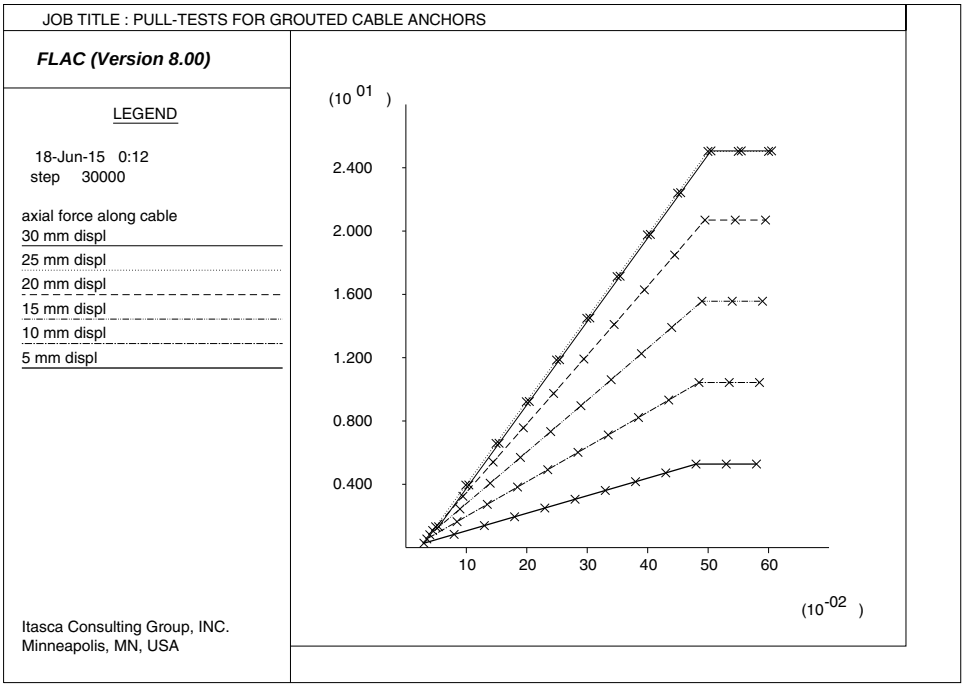

Figure 9.5 Evolution of the final axial force distribution (in tons/m) for a pull-test simulation on 26 mm cables in a single borehole. (Note that the last three points in each table are outside the grid and should be neglected.)

The cable shear bond strength will, in general, increase with increasing effective pressure p' acting on the cable. A linear law is implemented in *FLAC*, whereby the cable shear bond strength is defined as a constant (**sbond**) plus the effective pressure on the cable multiplied by the cable perimeter (**perimeter**) times a friction angle (**sfriction**). This pressure dependence is activated automatically in *FLAC* by issuing the cable properties **perimeter** and **sfriction**. Note that, in this case, the input data for **sbond** must correspond to the shear bond strength in a cable pull-out test carried out without confining pressure. Numerical results of pull-out tests on the 15.2 mm cable are presented for a friction angle of 20° and three levels of initial confining pressure, namely $p' = 10^5$, 10^6 and 10^7 N/m^2, in Figures 9.6 to 9.8. Those figures indicate an increasing failure level with increasing initial confining pressure, illustrating the frictional character of the cable-rock interface.

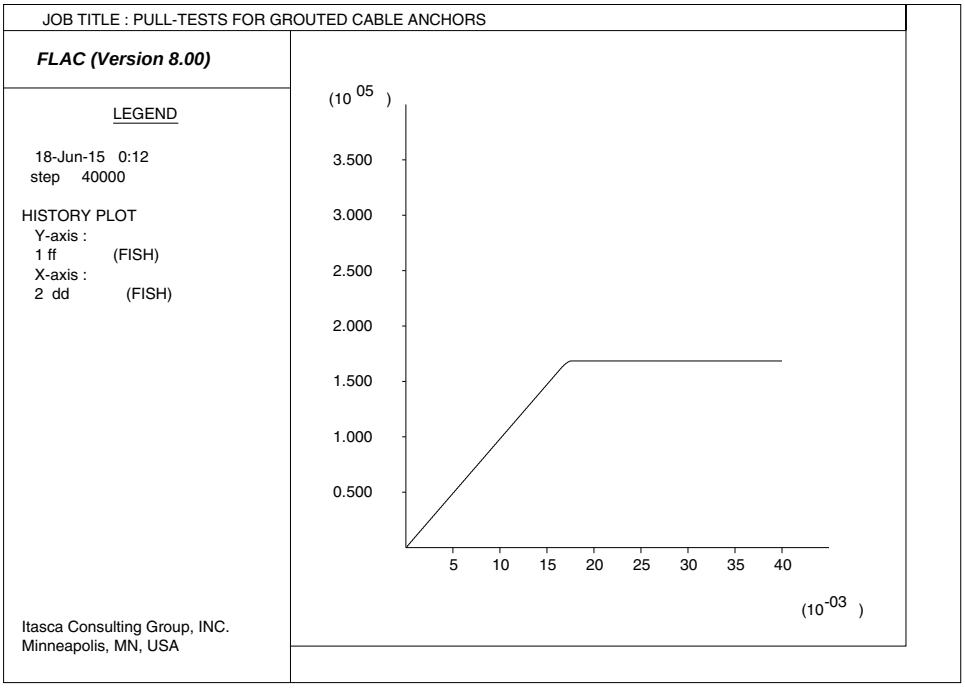

Figure 9.6 Pull-out test on 15.2 mm cable – $p = 10^5$ N/m^2

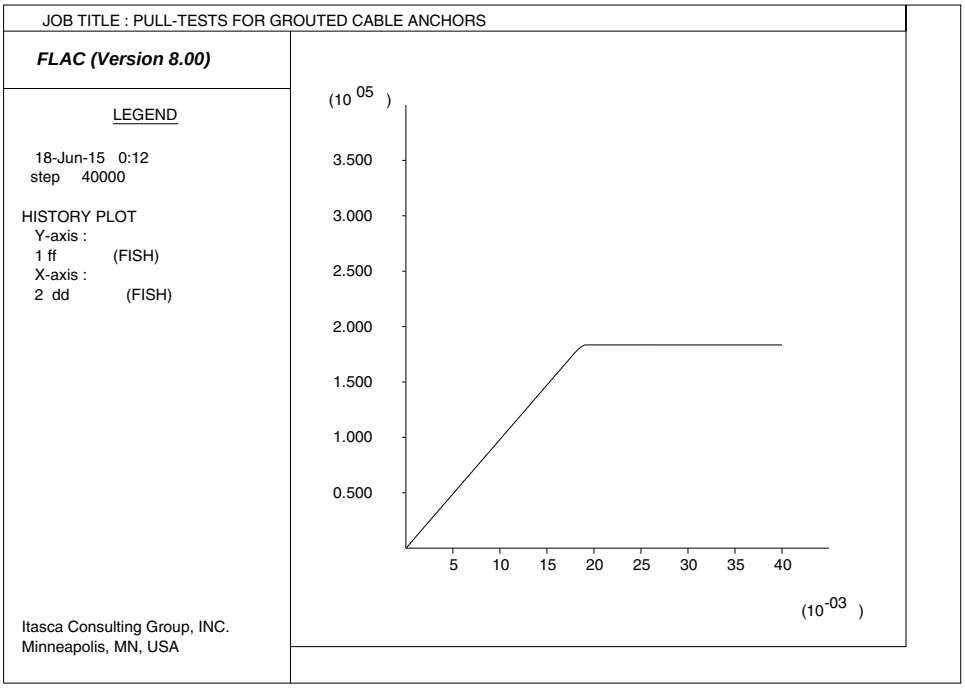

Figure 9.7 Pull-out test on 15.2 mm cable – $p = 10^6$ N/m^2

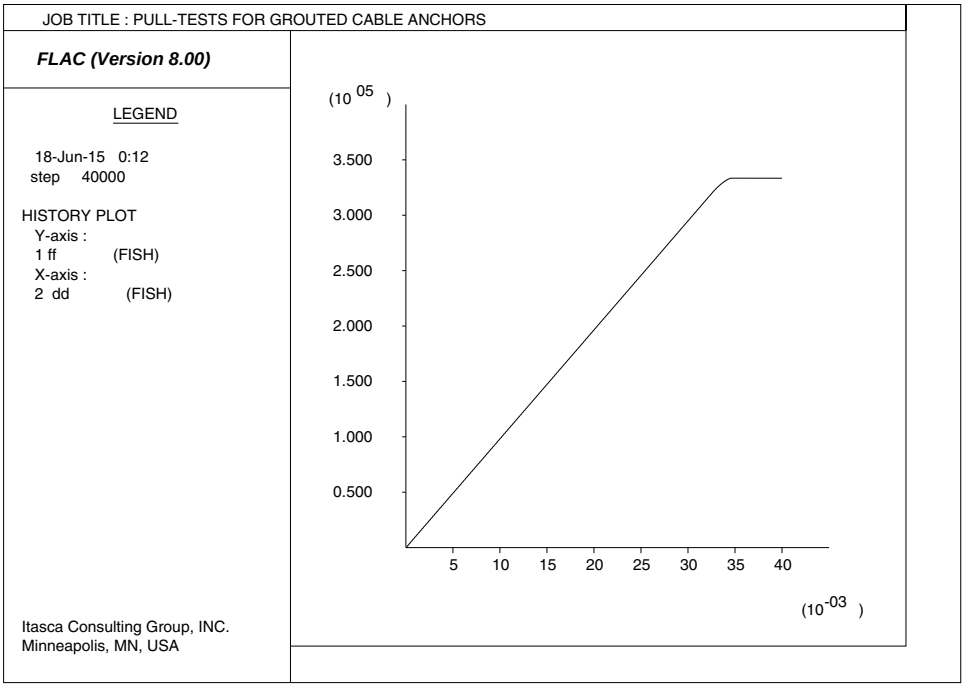

Figure 9.8 Pull-out test on 15.2 mm cable – $p = 10^7$ N/m^2

9.3 References

Hyett, A. J., W. F. Bawden and R. D. Reichert. "The Effect of Rock Mass Confinement on the Bond Strength of Fully Grouted Cable Bolts," *Int. J. Rock Mech. Min. Sci. & Geomech. Abstr.*, ***29***(5), pp. 503-524, 1992.

Kaiser, P. K., M. Diederichs and S. Yazici. "Cable Bolt Performance During Mining Induced Stress Change – Three Case Examples," in ***Rock Support in Mining and Underground Construction (Proceedings of the International Symposium on Rock Support, Sudbury, Ontario, Canada, June 1992)***, pp. 377-384. P. K. Kaiser and D. R. McCreath, eds. Rotterdam: A. A. Balkema (1992).